provide an accurate extrapolation.) This freedom in choosing the time step makes it possible to simulate narrow band behavior of materials for a longer period than possible with other time-domain methods like conventional, conditionally stable finite difference methods.

REFERENCES

[1] R. Mittra, "Transient electromagnetic fields," in *Topics in Applied Physics*, L. B. Felson and C. E. Baum, Eds. New York: Springer Verlag, 1976, vol. 10.

[2] C. L. Bennett, "A technique for computing approximate impulse response for conducting bodies," in *Electrical Engineering*. West Lafayette: Purdue Univ., 1968.

[3] B. Shanker, A. A. Ergin, and K. Aygün, "Analysis of transient electromagnetic scattering from closed surfaces using a combined field integral equation," *IEEE Trans. Antennas Propag.*, vol. 48, no. 7, pp. 1064–1074, Jul. 2000.

[4] B. P. Rynne, "Time domain scattering from arbitrary surfaces using the electric field integral equation," *J. Electromagn. Waves Applicat.*, vol. 5, no. 1, pp. 93–112, 1991.

[5] B. P. Rynne and P. D. Smith, "Stability of time marching algorithm for the electric field integral equation," *J. Electromagn. Waves Applicat.*, vol. 4, no. 12, pp. 1181–1205, 1990.

[6] J. J. Knab, "Interpolation of band-limited functions using the approximate prolate series," *IEEE Trans. Inf. Theory*, vol. 25, no. 6, pp. 717–720, 1979.

[7] D. S. Weile, G. Pisharody, N.-W. Chen, B. Shanker, and D. S. Weile, "A novel scheme for the solution of the time-domain integral equations of electromagnetics," *IEEE Trans. Antennas Propag.*, vol. 52, no. 1, pp. 283–295, Jan. 2004.

[8] L. E. Franks, *Signal Theory*. Stroudsburg, PA: Dowden & Culver, 1981.

[9] B. P. Lathi, *Modern Digital and Analog Communication Systems*. Oxford, U.K.: Oxford Univ. Press, 1998.

Enhancing the PML Absorbing Boundary Conditions for the Wave Equation

Yotka S. Rickard and Natalia K. Nikolova

***Abstract*—The dynamics of wave propagation and interactions in general media is described either by the system of Maxwell's equations, or by the wave equation. This paper focuses on problems modeled by the scalar wave equation, with one or more boundaries at infinity. The computational domain is truncated by a perfectly matched layer (PML) absorbing boundary condition (ABC) modified specifically for wave-equation applications. A problem independent approach is used to enhance the PML performance within the whole frequency band of excitation, in the presence of both evanescent and propagating fields. Numerical reflections below 0.1% are achieved with PML thickness of only six to eight cells, in both open and guided-wave problems.**

***Index Terms*—Absorbing boundary conditions (ABC), finite-difference time-domain (FDTD) methods, perfectly matched layer (PML), wave equation.**

I. INTRODUCTION

In time-domain electromagnetics, apart from the finite-difference time-domain (FDTD) method [1], an attractive new alternative is using the wave equation, as in the time-domain wave-potential (TDWP) method [2]. It employs only two scalar quantities, the magnitudes of two collinear vector potentials $(A, F)\hat{\xi}$, to analyze an EM problem in a region of distinguished axis $\hat{\xi}$ coparallel with the vector potentials. The propagation of the vector potentials is governed by three-dimensional (3-D) scalar wave equations. Two scalar quantities (and their first derivatives) are computed and stored at each time step, instead of the six quantities in Yee's FDTD method. This leads to substantial computer time and storage savings. Moreover, it leads to improved accuracy of the numerical algorithms because of the smoother behavior of the wave potentials in comparison with the field intensity vectors.

Both FDTD and TDWP methods require reliable and efficient ABCs for problems with boundaries at infinity. The perfectly matched layer (PML) ABC, introduced by Berenger [3] for Yee's FDTD method, is widely accepted as one of the most efficient numerical absorbers. Recently, corresponding PML ABC has been developed also for wave-equation applications [4], [5].

Much effort has been devoted toward improving and optimizing the performance of PML ABCs (see, e.g., [6]–[20]). Nevertheless, the active research continues, since even small numerical reflection in the time-domain response degrades the frequency-domain results, which are commonly used in microwave and antenna design.

The overall performance of the PML absorbing medium depends on the combined and interdependent influence of all its variables: the conductivity $\sigma_i (i = x, y, z)$, the loss factor α_i, the reflection coefficient R_0 and its thickness δ_i. Recently it was shown ([5], [20]) that if the conductivity and the loss factor grow at different exponent rates (which adds a new degree of freedom in their definition), the PML performance improves over the whole frequency band of interest. In [5], the conductivity is proposed to grow faster than the loss factor for the TDWP method. In [20], an enhanced PML performance is achieved within Yee's FDTD method. There, it is shown that in the presence of strong evanescent fields, the PML loss factor should grow faster than the PML conductivity.

In this communication, we show that similar enhancement of the PML performance can be achieved in wave-equation applications, without any increase in the computational load. In fact, greatly reduced PML thickness is used in comparison with the quoted in the literature, even when sources and/or discontinuities are located at two or three spatial steps from the PML interface.

First, half-a-cell displacement of the PML interface with the internal computational domain is proposed, so that any PML interface passes through the position of the vector component in all directions. With that, the whole PML medium is shifted in the corresponding direction by half a step. Second, the performance of few shifted PML ABCs, applied within the TDWP algorithm, are compared: Berenger's PML [3], the modified PML (MPML) [6], the generalized PML (GPML) [7], and the PML proposed in [5]. We demonstrate that all types of PML have significantly better performance when shifted. In 3-D open problems the PML proposed in [5] offers lower reflection levels in the entire frequency spectrum of interest. In guided-wave problems the PML proposed in [5] has lower reflection levels in comparison with the PMLs with real stretch of their parameters. A complex stretch of the PML parameters, such as in the FDTD complex-frequency-shifted (CFS) PML [13], [15]–[17], may lead to even lower reflections of evanescent modes. However, its implementation with the wave equation is far from trivial and will be addressed elsewhere. We investigate the influence of the difference β between the growth rates of the conductivity and the loss factor of the shifted wave equation PML. Based on extensive numerical experiments, practical recommendations for the choice of the PML parameters are offered.

Manuscript received March 9, 2004; revised September 1, 2004.

The authors are with the Department of Electrical and Computer Engineering, McMaster University, Hamilton, ON L8S 4K1, Canada (e-mail: yotka@ece.mcmaster.ca).

Digital Object Identifier 10.1109/TAP.2004.842584

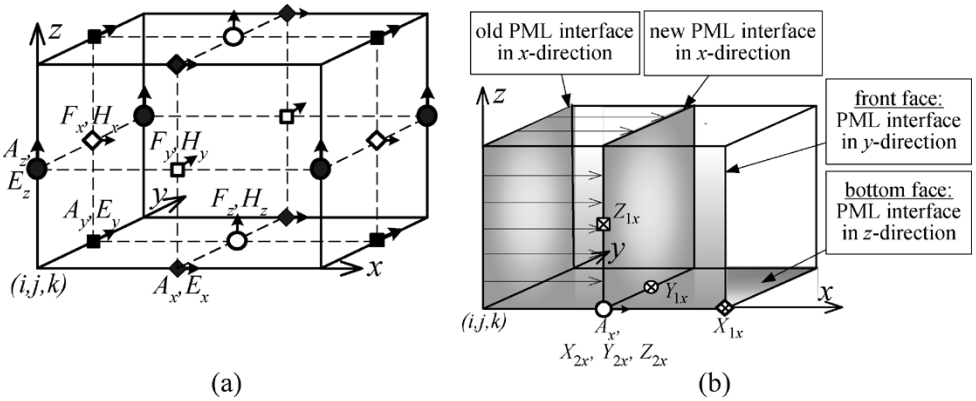

Fig. 1. (a) The (i, j, k)th numerical cell showing the corresponding component positions of the vector potentials in the TDWP method and the field intensity vectors in the FDTD method. (b) The (i, j, k)th numerical cell showing the positions of the x-component of the vector potential A_x, its corresponding auxiliary variables and the PML interfaces.

II. Theory

Berenger's PML [3] added a new degree of freedom to the FDTD algorithm to ensure the absorption of all *propagating* waves. To accelerate the attenuation rate of *evanescent* modes, Chen *et al.* [6] proposed the MPML, where another degree of freedom is added by including a PML loss factor α_i. In [5], a PML ABC is developed for the 3-D scalar wave equation, although a thick (20-layer) absorber is used. There, the PML conductivity and loss factor grow at different exponent rates. Thus a new degree of freedom in their definition is added. The PML conductivity profile σ_i grows at a higher rate than that of the PML loss factor α_i

$$\sigma_i(\rho) = \sigma_{\max}\left(\frac{\rho_i}{\delta_i}\right)^{n+\beta} \qquad \beta \in (0,3],\ i = x, y, z \tag{1}$$

while the PML loss factor α_i proposed by Chen *et al.* [6] remains

$$\alpha_i(\rho) = 1 + \varepsilon_{\max}\left(\frac{\rho_i}{\delta_i}\right)^{n} \qquad i = x, y, z. \tag{2}$$

The PML is terminated by a PEC wall and therefore the expected reflection error at normal incidence is

$$R_0 = \exp\left(-\frac{2}{\varepsilon_0 c}\int_0^{\delta}\sigma_i(\rho)d\rho\right). \tag{3}$$

Hence, in (1), the parameter $\sigma_{\max}$ controlling the rate of attenuation of propagating waves is

$$\sigma_{\max} = -\frac{(n+\beta+1)\varepsilon_0 \cdot c \cdot \ln R_0}{2\delta_i} \qquad i = x, y, z. \tag{4}$$

Therein

R_0	user-defined reflection coefficient at normal incidence, in the range $R_0 \in [10^{-10}, 10^{-2}]$;
δ_i	thickness of the PML in the i-direction, $i = x, y, z$;
ρ_i	depth in PML, $0 \le \rho_i \le \delta_i$;
$\varepsilon_{\max}$	user-defined parameter, regulating the rate of the evanescent-mode attenuation, in the range $\varepsilon_{\max} \in [0, 15]$;
n	user-defined exponent rate of growth, usually in the range $n \in [2, 6]$;
β	user-defined difference in the growth rates of the PML conductivity and the PML loss factor, usually in the range $\beta \in [-3, 3]$;
ε_0	permittivity of vacuum;
c	speed of light.

In [5], the parameter β has only positive values and no evanescent fields are considered. In this communication, we also use negative values of β when strong evanescent fields are present, as in the FDTD applications in [20].

The PML outlined above can be viewed as a modification of the GPML [7], where the PML loss factor and PML conductivity have different profiles. In GPML, the PML loss factor α_i grows as in (2) and the PML conductivity is

$$\sigma_i(\rho) = \sigma_{\max_G}\alpha_i(\rho)\sin^2\left(\frac{\rho_i}{\delta_i}\right) \qquad i = x, y, z. \tag{5}$$

In (5), for the coefficient $\sigma_{\max_G}$ we have developed the recursive formula

$$\sigma_{\max_G}(n) = -\frac{\varepsilon \cdot c \cdot \ln R_0}{\delta_i\left[1 + \varepsilon_{\max}\left(\frac{1}{n+1} + \Sigma_n\right)\right]} \qquad i = x, y, z \tag{6}$$

where (for integer n)

$$\Sigma_n = \frac{n}{\pi^2}[1 + (n-1)\Sigma_{n-2}] \qquad n \ge 3$$
$$\Sigma_1 = \Sigma_2 = \frac{2}{\pi^2}. \tag{7}$$

Two modifications of the PML ABC implementation for the wave equation are proposed.

First, the location of the interface plane between the internal computational domain and the PML medium is proposed to pass through the position of the calculated variable *in all directions*. In the TDWP method, the positions of the magnetic vector potential components coincide with the positions of the electric field components within the conventional Yee's cell, namely, they are located at the middle of the edges of the numerical cell, see Fig. 1(a). Similarly, the positions of the electric vector potential components coincide with the positions of the magnetic field components within Yee's cell, namely, they are located at the middle of the cell faces. Thus, for example, for the x-component of the magnetic vector potential, $\vec{A} = \hat{x}A_x$, the position of the PML interface in the x-direction is proposed to pass through the middle of the numerical cell in the x-direction, and to remain unchanged in the other two directions, see Fig. 1(b). In the FDTD method, the PML interfaces pass through the faces of the numerical cells in all directions. However, the PML absorption for wave-equation applications is performed in two steps and requires two sets of auxiliary variables, see [5]. If the PML interfaces for the wave equation are located as in the PMLs for the FDTD method, as done in [5], the auxiliary variables are not equally absorbed in 3-D applications. Consequently, very thick absorbers are necessary, as shown in [5], where it is reported that even

with twenty-layer PMLs surrounding an infinitesimal dipole, the numerical reflections at low frequencies remain above 1%.

Second, the above modification requires a change of the location of the PML-terminating perfect-electric-conductor (PEC) wall in the corresponding direction, so that the whole PML medium is shifted by half-a-cell. For example, the half-a-cell displacement in the x-direction for A_x requires the PML-terminating PEC wall in the x-direction (Neumann BC) to be also displaced by half-a-cell. Therefore, it is implemented as the one-sided normal numerical derivative of second-order accuracy

$$\left.\frac{\partial A_x}{\partial x}\right|_{x=x_{\max}} = 0 \Rightarrow A_x(x_{\max}) = \frac{4A_x(x_{\max}-\Delta x) - A_x(x_{\max}-2\Delta x)}{3\Delta x}. \quad (8)$$

At the tangential PML-terminating PEC planes (Dirichlet BC) in the y-and z-directions, the vanishing A_x conditions remain

$$A_x|_{y=y_{\max}} = 0 \quad \text{and} \quad A_x|_{z=z_{\max}} = 0. \quad (9)$$

Corresponding expressions hold at $x = x_{\min}$, $y = y_{\min}$, and $z = z_{\min}$.

The actual scheme for calculating the conductivity and the loss factor inside the PML medium is based on the usual spatially polynomial scaling as in (1) and (2), where the distance ρ_i is measured now from the new position of the PML interface.

Having in mind that the positions of the vector potentials and field intensities coincide, as shown in Fig. 1(a), it is clear that this half-a-cell shift of the PML medium is directly applicable for any wave equation, regardless of its specific variable—potential or field intensity.

III. Numerical Results and Discussion

To illustrate the performance of the proposed PML ABC for wave-equation applications, three examples are considered: an infinitesimal dipole in open space, a dielectric slab, and a rectangular waveguide. They are modeled by the TDWP method. The reflection magnitude is estimated using the ratio of the reflected and incident wave-potential component g_i, which has been excited

$$R = \left| \frac{\mathfrak{F}\{g_i^{\text{refl}}\}}{\mathfrak{F}\{g_i^{\text{inc}}\}} \right| \quad (10)$$

Here, $\mathfrak{F}$ denotes Fourier transform of the respective time-domain wave-potential component.

A. Dipole in Open Space

The infinitesimal dipole in open space is modeled in a computational domain of $(130\Delta x, 130\Delta y, 130\Delta z)$, where $\Delta x = \Delta y = \Delta z = 0.75$ mm. The magnetic potential $\vec{A} = \hat{x}A_x$ is excited by the x-directed current of the dipole, which is a Gaussian pulse in time. Fig. 2 shows a comparison of the proposed PML ($\beta = 1$) with Berenger's PML [3], the GPML [7], and the MPML [6]. The PML interfaces and PEC terminating walls of all four types of PML ABCs have locations modified as described above. For each type of PML the optimal parameterization is used, based on data from the literature and on extensive numerical experiments. A very long simulation time is used so that not only the direct reflections from the PMLs but also the interferences from the reflections are included. Here, we should emphasize that the results presented in Fig. 2 are for six-layer PML ABCs. Nevertheless, the reflection level for all types of PML is an order of magnitude lower than that for the twenty-layer PML ABCs reported in [5]. The PML profile with $\beta > 0$ offers a reflection level of about 0.01% (−80 dB) *in the whole frequency band* of the excitation. The proposed interface shift leads to an unprecedented reduction in the PML thickness, while retaining excellent performance.

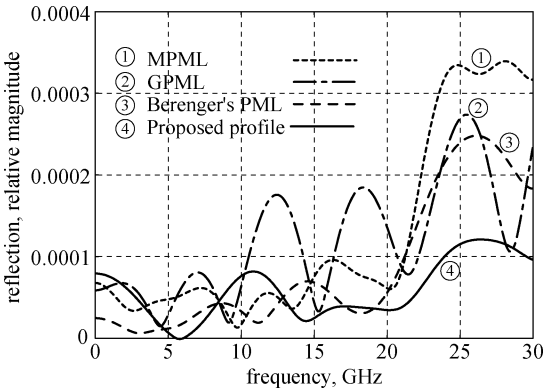

Fig. 2. Infinitesimal dipole in open space for PML thickness $N_{\text{PML}} = 6$. In Berenger's PML: $R_0 = 10^{-6}$, $\varepsilon_{\max} = 0$, $n = 3.5$. In MPML: $R_0 = 10^{-6}$, $\varepsilon_{\max} = 1$, $n = 3.5$. In GPML: $R_0 = 10^{-4}$, $\varepsilon_{\max} = 1$, $n = 4$. In the proposed PML: $R_0 = 10^{-4}$, $\varepsilon_{\max} = 1$, $n = 2.5$, $\beta = 1$.

B. Dielectric Slab in Open Space

The dielectric slab is considered to investigate the influence of material interfaces intersecting the PML boundaries. Its thickness is 10 mm and the dielectric constant is $\varepsilon_r = 4$. It is excited by a vertical infinitesimal dipole buried in its center, five spatial steps after the front-end PML. The magnetic potential $\vec{A} = \hat{x}A_x$ is excited by the x-directed dipole current, which is a sinusoidal wave of frequency $f_0 = 7.5$ GHz modulated by Blackman-Harris window (BHW) function [21] giving a frequency bandwidth from 5.5 GHz to 9.5 GHz. The computational domain $(170\Delta x, 34\Delta y, 39\Delta z)$ is surrounded in all six directions by the PML medium. Uniform mesh with $\Delta x = \Delta y = \Delta z = 2$ mm is used. The interface between the internal computational domain and all types of PML medium is shifted as described in Section II. Fig. 3 shows the numerical reflections from the proposed PML with $\beta = 1.5$, from Berenger's PML, from the GPML and from the MPML. The sample plane is 40 steps away from the excitation so that there is a sufficient time guard to separate the incident and the reflected pulse. The PML thickness is $N_{\text{PML}} = 6$ cells. The nearly optimal parameterization for each PML type is used using data from the available literature and numerical experiments. Although not shown in the figure, the numerical reflections without the interface shift are an order of magnitude higher for all PML types. Fig. 3 shows that with the proposed interface shift, only six-cell thick PMLs can ensure numerical reflections of about 0.1% of the magnitude of the incident wave in the whole frequency band of the excitation.

C. Evanescent and Propagating Waves in a Waveguide

Finally, a hollow rectangular waveguide of cross section of 30 mm by 15 mm (cutoff frequency 5 GHz) is considered. It is excited by a current sheet, which is a sinusoidal wave of frequency 7 GHz modulated by BHW function [21], so that its frequency content is from 0 to 14 GHz. Uniform mesh with $\Delta x = 1.25$ mm is used. The excitation plane is 40 steps after the front-end PML, which is 30 cells thick. To properly measure the reflections associated with evanescent waves, the sampling location is only one spatial step after the excitation plane. The eight-cell thick back-end PML is located two spatial steps after the sampling plane. De-embedding with longer waveguide is performed. Very long simulation time (of the order of 10^5 time steps) is necessary, as noted in [22]. Because of the presence of evanescent modes, a negative value of the parameter β is used. Fig. 4 shows a comparison of the numerical reflections from the proposed PML ($\beta = -0.7$) with those

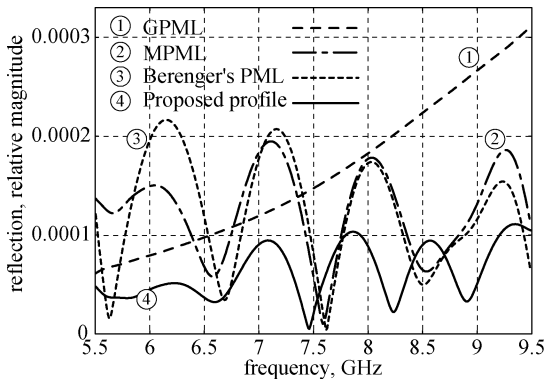

Fig. 3. Dielectric slab—numerical reflections with $N_{\rm PML} = 6$ cells. In Berenger's PML: $R_0 = 10^{-8}$, $\varepsilon_{\max} = 0$, $n = 3.5$. In MPML: $R_0 = 10^{-8}$, $\varepsilon_{\max} = 1$, $n = 3.5$. In GPML: $R_0 = 10^{-4}$, $\varepsilon_{\max} = 1$, $n = 2$. In the proposed PML: $R_0 = 10^{-4}$, $\varepsilon_{\max} = 1$, $n = 2$, $\beta = 1.5$.

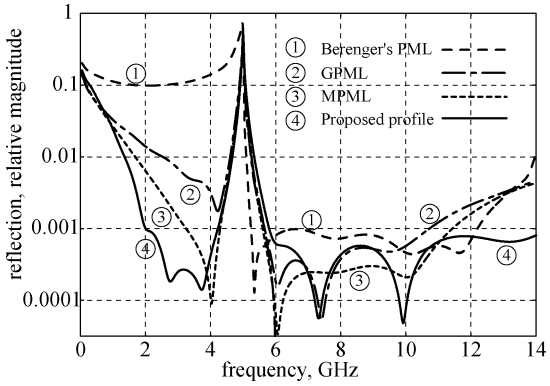

Fig. 4. Evanescent and propagating waves in rectangular waveguide with 8-cell PMLs. In Berenger's PML: $R_0 = 10^{-12}$, $\varepsilon_{\max} = 0$, $n = 2$. In GPML: $R_0 = 10^{-4}$, $\varepsilon_{\max} = 10$, $n = 4$. In MPML: $R_0 = 10^{-4}$, $\varepsilon_{\max} = 10$, $n = 3$. Proposed profile: $R_0 = 10^{-4}$, $\varepsilon_{\max} = 10$, $n = 2.4$, $\beta = -0.7$.

from Berenger's PML, the GPML, and the MPML. The best possible parameterization is used for each type of PML, based both on data from the available literature and on numerical experiments.

The reflection from the eight-cell thick PML with negative β is comparable with the reflections from 16-cell-thick Berenger's PML and GPML [7], [22]. We again note that the use of CFS PML [15]–[17] might lead to better absorption at the lowest end of the frequency band, as all PMLs with real stretches of their parameters do not absorb well at very low frequencies.

It is noticed that increasing the value of the parameter $\varepsilon_{\max}$ in the loss factor α_i improves the evanescent wave attenuation (as expected) but leads to higher numerical reflections after the cutoff frequency and especially toward the high end of the frequency band. This is a common drawback of all PML absorbers, which employ $\alpha_i > 1$. On the other hand, the numerical experiments show that decreasing R_0 has exactly the opposite effect. The negative value of β balances these competing influences and ensures lower numerical reflections in comparison with the PML implementations with real stretches of the PML parameters. With negative β, we observe that if we choose $R_0 = 10^{-m}$, for any $m \in [3, 10]$, then the choice $\varepsilon_{\max} = 2.5$ m ensures the lowest reflections both before and after the cutoff frequency, below 0.1% up to the high end of the frequency band. The higher the value of m, the narrower the cusp around the cutoff frequency, as observed also in [16].

D. The Choice of the PML Parameters

It is well known that higher exponent rates of growth of the PML conductivity σ_i and PML loss factor α_i lead to faster absorption of the impingent waves but also give rise to higher numerical reflections due to the bigger jumps in their stepwise approximation. That is why, the smaller the PML thickness, the lower the maximum growth rate $n_{\max}$ of σ_i and α_i should be. On the other hand, with the polynomial scaling, the growth rate of σ_i and α_i is always $n_{\min} > 1$. The above considerations limit the possible range of values for the parameter β, which is the difference between the growth rates of σ_i and α_i. Therefore

$$|\beta| \leq n_{\max} - n_{\min} \tag{11}$$

where $n_{\max}$ and $n_{\min}$ are the maximum and minimum exponent rates for a given PML thickness. In practice, $n_{\min} > 1.5$, and as a rule-of-thumb, $n_{\max} \leq \min([N_{\rm PML}/2], 6)$. Thus, for a PML thickness of six or eight cells, best results are obtained when $0 < |\beta| < 2.5$ where

(i) β is positive in problems with little or no evanescent fields, and

(ii) β is negative in the presence of strong evanescent fields.

If thicker PML absorbers are used, higher values of β are possible.

To summarize, we choose the PML parameters as follows.

(i) To maintain the numerical reflections between 0.01% and 0.1% of the incident wave amplitude, the (theoretical) reflection coefficient is usually set to $R_0 = 10^{-4}$. In the presence of both evanescent and propagating fields, lower values of R_0 may be used for a narrower cusp around the cutoff frequency.

(ii) A minimal practical exponent rate of growth $1.7 \leq n \leq 2$ is used for σ_i in the presence of evanescent fields, and $n = 2$ for α_i otherwise.

(iii) For a PML thickness $N_{\rm PML} = 6$ or 8 cells, the maximum exponent rate of growth should not exceed $n = 4$, which allows for $|\beta| \leq 2.3$. If the PML interface is in close proximity of sources and/or discontinuities, the preferred choice is $0.5 \leq |\beta| \leq 1$.

(iv) In the definition of α_i, when strong evanescent fields are present, the coefficient $\varepsilon_{\max}$ is set to $\varepsilon_{\max} = 2.5$ m, following the choice of the reflection coefficient $R_0 = 10^{-m}$, $m \in [3, 10]$. In all other cases, it is set to $\varepsilon_{\max} = 1$.

IV. Conclusion

For wave equation applications, the interface between the internal computational domain and the PML absorber is proposed to pass through the positions of the scalar variable in all directions. This requires half-a-cell displacement of the interface (and the whole PML medium) in some directions and may require modified Neumann and/or Dirichlet BC at the PML-terminating PEC walls. Such PML-interface displacement enhances significantly the PML performance. In all major types of problems, a PML thickness as low as six to eight cells ensures reflections below 0.1% (−60 dB). Moreover, its performance does not deteriorate in close proximity of sources and/or discontinuities.

Where little or no evanescent energy is present, we recommend that the PML conductivity increases faster than the PML loss factor, i.e., $\beta > 0$. In the cases where both evanescent and propagating modes are present, a negative value of β balances the opposing influences of the other PML parameters. We also give procedure for a near optimal choice of the wave-equation PML parameters. Although examples with the TDWP method are shown, where the magnetic vector potential is

used, it is noted that the proposed PML ABC is applicable to any wave equation regardless of its specific variable.

REFERENCES

[1] K. S. Yee, "Numerical solution of initial boundary value problems involving Maxwell's equations in isotropic media," *IEEE Trans. Antennas Propag.*, vol. 14, no. 3, pp. 302–307, May 1966.

[2] N. K. Georgieva, "Construction of solutions to electromagnetic problems in terms of two collinear vector potentials," *IEEE Trans. Microwave Theory Tech.*, vol. 50, no. 8, pp. 1950–1959, Aug. 2002.

[3] J. P. Berenger, "A perfectly matched layer for the absorption of electromagnetic waves," *J. Comp. Physics*, vol. 114, no. 2, pp. 185–200, Oct. 1994.

[4] D. Zhou, W. P. Huang, C. L. Xu, and D. G. Fang, "The perfectly matched layer boundary condition for scalar finite-difference time-domain method," *IEEE Photon. Technol. Lett.*, vol. 13, no. 5, pp. 454–456, May 2001.

[5] Y. S. Rickard, N. K. Georgieva, and W.-P. Huang, "Application and optimization of PML ABC for the 3-D wave equation in the time domain," *IEEE Trans. Antennas Propag.*, vol. 51, no. 2, pp. 286–295, Feb. 2003.

[6] B. Chen, D. G. Fang, and B. H. Zhou, "Modified Berenger PML absorbing boundary condition for FD-TD meshes," *IEEE Microw. Guided Wave Lett.*, vol. 5, no. 11, pp. 399–401, Nov. 1995.

[7] J. Fang and Z. Wu, "Generalized perfectly matched layer for the absorption of propagating and evanescent waves in lossless and lossy media," *IEEE Trans. Microwave Theory Tech.*, vol. 44, no. 12, pp. 2216–2222, Dec. 1996.

[8] G. Lazzi and O. P. Gandhi, "On the optimal design of the PML absorbing boundary condition for the FDTD code," *IEEE Trans. Antennas Propag.*, vol. 45, no. 5, pp. 914–917, May 1997.

[9] E. Michielssen, W. C. Chew, and D. S. Weile, "Genetic algorithm optimized perfectly matched layers for finite difference frequency domain applications," in *IEEE Antennas Propag. Soc. Int. Symp. Dig.*, 1996, pp. 2106–2109.

[10] S. C. Winton and C. M. Rappaport, "Specifying PML conductivities by considering numerical reflection dependencies," *IEEE Trans. Antennas Propag.*, vol. 48, no. 7, pp. 1055–1063, Jul. 2000.

[11] L. Zhao and A. C. Cangellaris, "The generalized theory of perfectly matched layers (GT-PML): numerical reflection analysis and optimization," in *IEEE Antennas Propagat. Soc. Int. Symp. Dig.*, vol. 3, 1997, pp. 1896–1899.

[12] S. D. Gedney, "An anisotropic PML absorbing media for the FDTD simulation of fields in lossy and dispersive media," *Electromagnetics*, vol. 16, no. 4, pp. 399–416, Apr. 1996.

[13] M. Kuzuoglou and R. Mittra, "Frequency dependence of the constitutive parameters of causal perfectly matched anisotropic absorbers," *IEEE Trans. Microw. Guided Wave Lett.*, vol. 6, no. 12, pp. 447–449, Dec. 1996.

[14] S. Abarbanel and D. Gottlieb, "A mathematical analysis of the PML method," *J. Comput. Phys.*, vol. 134, pp. 357–363, 1997.

[15] J.-P. Berenger, "Evanescent waves in PML's: origin of the numerical reflection in wave-structure interaction problems," *IEEE Trans. Antennas Propag.*, vol. 47, no. 10, pp. 1497–1503, Oct. 1999.

[16] ——, "Application of the CFS PML to the absorption of evanescent waves in waveguides," *IEEE Microw. Wireless Components Lett.*, vol. 12, no. 6, pp. 218–220, Jun. 2002.

[17] J. A. Roden and S. D. Gedney, "Convolution PML (CPML): an efficient FDTD implementation of the CFS-PML for arbitrary media," *Microw. Opt. Tech. Lett.*, vol. 27, no. 5, pp. 334–337, Dec 2000.

[18] J. S. Juntunen, N. V. Kantartzis, and T. D. Tsiboukis, "Zero reflection coefficient in discretized PML," *IEEE Microw. Wireless Compon. Lett.*, vol. 11, no. 4, pp. 155–157, Apr. 2001.

[19] K. P. Prokopidis, N. V. Kantartzis, and T. D. Tsiboukis, "Performance optimization of the PML absorber in lossy media via closed-form expressions of the reflection coefficient," *IEEE Trans. Magn.*, vol. 39, no. 3, pp. 1234–1237, May 2003.

[20] Y. S. Rickard and N. K. Georgieva, "Problem-independent enhancement of PML ABC for the FDTD method," *IEEE Trans. Antennas Propag.*, vol. 51, no. 10, pp. 3002–3006, Oct. 2003.

[21] F. J. Harris, "On the use of windows for harmonic analysis with the discrete Fourier transform," *Proc. IEEE*, vol. 66, no. 1, pp. 51–83, Jan. 1967.

[22] C. E. Reuter, R. M. Joseph, E. T. Thiele, D. S. Katz, and A. Taflove, "Ultrawideband absorbing boundary condition of waveguiding structures in FD-TD simulations," *IEEE Microw. Guided Wave Lett.*, vol. 4, no. 10, pp. 344–346, Oct. 1994.